Beyond the Lenormand phase diagram: Self-regulation mechanisms for controlling two-phase flows in porous media

Xiaokang Guo[1,2,*]

[1]College of Civil Engineering and Architecture, Hebei University, Baoding, 071002, China

[2]Technology Innovation Center for Testing and Evaluation in Civil Engineering of Hebei Province, Hebei University, Baoding, 071002, China

*Corresponding author: guoxiaokang17@mails.ucas.edu.cn

Abstract

It is unclear why two-phase fluid flows in porous media develop a series of fluid displacement patterns. This study treats a two-phase flow system as an open thermodynamical system with a two-phase displacement process that follows the principle of the minimum operating power (MOPR). When different constraints are imposed on the system, the pore-scale interfacial dynamic response to this principle varies significantly, and a series of self-regulation mechanisms exist. These new findings not only explain the physical origins of the diverse fluid displacement patterns and interface reconstruction events but also provide new insights into the interface invasion protocol.

Plain Language Summary

Why do immiscible two-phase fluid flows in porous media have a range of different fluid distribution characteristics under different pore structures, fluid properties, and wettability conditions? Does their occurrence follow a relatively uniform control principle? This study demonstrated that the evolution direction of a two-phase flow system follows the principle of the minimum operating power (MOPR). During the two-phase displacement process, the system regulates itself through a series of self-regulation mechanisms to reduce the operating power. A series of fluid displacement patterns can be regarded as the minimum operating power states corresponding to a given displacement task under different system constraints, and the formation of these patterns is inevitable, thereby preventing extra work for the system. These

findings provide new insights for the control of the interface invasion protocol that underlies macroscopic flow properties.

Keywords: Displacement pattern; Minimum operating power principle; Self-regulation mechanisms; Interface reconstruction events

1. Introduction

Immiscible two-phase fluid flows in porous media are important processes in natural and engineered systems for carbon dioxide sequestration (CCS), enhanced oil recovery (EOR), and nonaqueous phase liquid (NAPL) remediation, among other applications (Singh et al., 2019; Holtzman and Segre, 2015; Zhao et al., 2016). The macroscopic flow properties are related to interfacial instabilities at the pore scale, and understanding the flow behavior at the pore scale is crucial for the optimal design of these processes. In the past few decades, to understand the complexity of multiphase flows in porous media, scholars have conducted many numerical and experimental studies to systematically explore the influencing mechanisms of various characteristics, such as the pore structure, fluid properties and wettability, on two-phase flows (Jiang et al., 2015; Zacharoudiou et al., 2020; Rokhforouz et al., 2019). At present, most studies on two-phase displacement are conducted based on the Lenormand phase diagram and are mainly from the perspective of force equilibrium, and the flow pattern dominating a given displacement process can be determined by comparing the relative importance of gravity, the viscous force, and the capillary force (Lenormand et al., 1988).

When gravity is negligible, the dynamics governing the fluid displacement pattern can be characterized by two dimensionless numbers, namely, the capillary number (Ca = $\mu_i v_i / \sigma$) and the viscosity ratio (M = μ_i / μ_d), where v is the characteristic velocity, σ is the surface tension coefficient, μ is the viscosity coefficient, and the subscripts i and d represent the invading phase and the displaced phase, respectively. When Ca is large and M < 1, the viscous force dominates over the capillary force, and the fluid–fluid interface develops dendritic structures along the flow direction, which is called viscous fingering (VF). In contrast to M < 1, in the case of favorable viscosity (M > 1), the displacement front is viscous stable, and the invading fluid scans the porous medium compactly, forming a stable

displacement (SD). For low Ca, the capillary force dominates over the viscous force, and an intermittent fluid displacement process, called capillary fingering (CF), is observed. The transition mode between these patterns is called a crossover zone (CZ).

In addition, wettability also plays an important role in the two-phase displacement process. For example, Cieplak and Robbins (1990) proposed three modes of meniscus motion (referred to as interface reconstruction events), namely, burst, contact, and overlap, and they elucidated pore-scale displacement events at different wettabilities. Since then, in the spirit of the Cieplak and Robbins model, the complex interactions between wettability and pore geometry, along with the flow conditions, have been further investigated, thereby extending the Cieplak-Robbins description of quasistatic fluid invasion and effectively extending the classic Lenormand phase diagram (Basirat et al., 2017; Lin et al., 2021; Jahanbakhsh et al., 2021; Jung et al., 2016; Hu et al., 2018). Clearly, the obtained Lenormand phase diagram and related extended phase diagram based on the analysis of the force equilibrium provide important insights into the dynamics of immiscible fluid displacement in porous media. However, these studies did not fully elucidate the pore-scale flow physics behind complex two-phase flow systems. For example, although transient dynamics during interface reconstruction events have been extensively studied (Chen et al., 2019; Zacharoudiou et al., 2016), it is generally believed that these events violate the hypothesis of slow displacement and are a fast and irreversible process leading to energy dissipation. For example, Berg et al. (2013) conducted energy conversion analysis based on 3D micro CT data and found that 64% of the pressure volume work was dissipated through the Haines jump event. Hu et al. (2018) analyzed the basic relationship between displacement mode conversion and energy conversion in rough fracture two-phase flow. In the capillary state, approximately 51-58% of the surface energy is dissipated by irreversible events. However, we believe that previous explorations of the argument that the interface reconstruction event is an adverse energy mechanism have been insufficiently rigorous. Among them, the physical origin of a series of fluid displacement patterns or a series of interface reconstruction events is still unclear, and it is unknown if such patterns and events follow a relatively unified control principle. Obviously, the previous

arguments based on the competition among the viscous force, capillary force and gravity cannot provide a convincing physical explanation, and a new criterion is needed to study immiscible displacement dynamics.

Based on the theory of nonequilibrium thermodynamics, in the linear nonequilibrium region, an irreversible process in an open system always develops in the direction of decreasing entropy production rate until the system reaches a nonequilibrium steady state that satisfies the constraints. At this time, the entropy production rate is minimal under the external constraints, which is called the principle of the minimum entropy production rate (MEPR). The MEPR indicates the development and evolution direction of a dynamical system, that is, no matter what its initial motion state is, if the system deviates from a stable nonequilibrium state, its entropy production rate is not minimal, and the system must adjust by reducing the entropy production rate until the entropy production rate reaches the minimum and the system returns to a steady state. The MEPR has been demonstrated to be very successful in explaining natural phenomena in both classical and modern physics (Xu et al., 2016; Huang et al., 2004; Nanson et al., 2008; Jansen et al., 2004). According to Nanson et al. (2008), rivers are natural "machines" that consume energy to perform work. In river systems with surplus energy, the surplus energy can be consumed by adjusting the flow wave characteristics and area. Xu et al. (2016) deduced the principle of the minimum energy dissipation rate (MEDR) from the MEPR and verified the validity of the MEDR for alluvial rivers using field data. When a river system is in a state of relative equilibrium, its energy dissipation rate is minimal. Clearly, the MEPR, as a universal principle, is also applicable to the field of two-phase flow in porous media.

For two-phase flow systems in porous media, although an immiscible fluid flow often exhibits complex nonlinear behavior, unsteady turbulence is usually not involved; hence, two-phase flow systems can be treated as linear nonequilibrium thermodynamic systems. A two-phase displacement process follows not only the law of conservation of energy but also the MEPR. However, in contrast to the fluvial dynamics systems described above, when two-phase flows are involved, the presence of phase interfaces leads to a discontinuous fluid distribution

and a more complex energy balance field. Energy conversion usually occurs among the surface energy, pressure–volume work, kinetic energy and dissipated energy, and the MEPR is not simply equivalent to the MEDR. In this study, we found that the evolution direction of the fluid displacement pattern follows a relatively unified control principle, that is, the principle of the minimum operating power (MOPR). In addition, by clarifying the self-regulation mechanism derived by the system that follows the MOPR principle, the physical origins of the diversity of fluid displacement patterns can be explained.

2. Flow patterns and analysis

2.1. Principle of the minimum entropy production rate

In the context of the MEPR, in thermodynamics, an open system uses the least possible energy to accomplish a given task, which includes constant single-phase flow and two-phase displacement tasks. For a steady-state viscous single-phase flow, the system is in a stable nonequilibrium state. In this paper, a principle equivalent to the MEPR is proposed, namely, the MOPR. Specifically, in a control volume Ω with open boundaries, when a fluid flows in at a constant flow rate Q (isothermal system), the operating power of the system can be described as $P_o = \Delta pQ = \Phi$; that is, the power derived from the inlet and outlet pressure difference $\Delta p = p_{\text{int}} - p_{out}$ through the system boundary is equal to the viscous dissipation rate of the system Φ integrated over the entire porous domain (i.e., the entropy production rate). The operating power P_o is clearly limited by the static constraints of the system (including the pore structure, fluid properties, and boundary conditions, among others) and is always minimal under the given constraints ($P_o = P_{\min}$).

Although the evolution direction of a two-phase flow system still follows the MOPR, the process of two-phase displacement includes both static and dynamic system constraints (that is, the topology of the two-phase fluid). Even if the static constraints of the system remain unchanged, the fluid topology is always undergoing a dynamic evolution process, causing the system to deviate from a stable nonequilibrium state and the operating power P_o to no longer be minimal, and the system develops in the direction of reduced operating power. Due

to the change in the fluid topology, the corresponding minimum operating power $P_{\min}$ is no longer constant and may increase or decrease. Furthermore, compared to the simple energy conversion relationship of a steady-state single-phase flow system, the two-phase displacement process involves more energy terms, including pressure–volume work, surface energy, dissipated energy, and kinetic energy terms. The conversion form of the system operating power P_o changes significantly and is no longer equal to the viscous dissipation rate Φ. For an isothermal irreversible drainage process, the system operating power can be described as

$$P_o = \Phi + \frac{dF_{surf}}{dt} + \frac{dE}{dt} \tag{1}$$

In Equation (1), the rate of energy introduction P_o into the system by the external pressure difference is equal to the sum of the viscous dissipation rate Φ, the rate of change in the surface energy dF_{surf}/dt, and the rate of change in the bulk kinetic energy dE/dt of the system. Among them, the viscous dissipation rate Φ of the system consists of the viscous dissipation rate of the invading phase Φ_i, the viscous dissipation rate of the displaced phase Φ_d, and the additional viscous dissipation rate due to inertial effects (inertial dissipation rate) Φ_n in the calculation domain. When inertial effects are not considered, Φ_n can be ignored. The rate of change in the surface energy dF_{surf}/dt consists of the rate of change in the solid-liquid surface energy $dF_{surf-s}/dt = \left|\cos\theta^{eq}\right|\sigma dA_{ns}/dt$ and the rate of change in the liquid-liquid surface energy $dF_{surf-f}/dt = \sigma dA_{\text{int}}/dt$, where A_{ns} is the nonwetting phase-solid interfacial area, and A_{int} is the fluid–fluid interfacial area. $dE/dt = \int_{\Omega} \frac{1}{2}\rho \mathbf{v}\cdot\mathbf{v} d\Omega \Big/ dt$ is the rate of change in the bulk kinetic energy, which consists of the rate of change in the kinetic energy of the invading phase dE_i/dt, the rate of change in the kinetic energy of the displaced phase dE_d/dt, and the rate of change in the kinetic energy of

the fluid phase discharged through system outlets dE_f/dt in the calculation domain. Coupling effects exist among Φ, dF_{surf}/dt and dE/dt, and a change in one energy term inevitably causes fluctuations in other energy contribution terms. As a result, different energy terms contribute differently when the system approaches the minimum operating power state ($P_o \to P_{\min}$) under different constraints. Therefore, in contrast to the case of a steady-state single-phase flow with no self-regulation mechanism, in the two-phase fluid displacement process, the interface dynamics respond to the MOPR to derive a self-regulation mechanism. The system regulates itself through this self-regulation mechanism to reduce the operating power ($P_o \to P_{\min}$). Under different constraints, the regulation mechanism for avoiding extra work could be different and mainly depends on which energy contribution term is most beneficial for controlling the system to approach the minimum operating power state.

2.2. Self-regulation mechanisms

To analyze a series of self-regulation mechanisms that govern interface dynamics and fluid displacement patterns, a series of two-phase flow numerical simulations using a digital core model are performed. A digital core model of the microscopic pore structure is established by using computed tomography (CT), and the coupled Navier-Stokes and Cahn-Hilliard equations are solved using the finite element method (with COMSOL Multiphysics software) to capture the dynamic evolution of the flow front. For more details on CT image processing and the phase field method (PFM), please refer to our previous work (Guo et al., 2020). The main numerical results are presented in the form of a visual phase diagram of the fluid distribution at breakthrough in a log Ca-log M plot, as shown in Fig. 1. As Ca increases, the fluid displacement pattern changes from capillary fingering to viscous fingering (M <1) or stable displacement (M>1). From the perspective of the Lenormand phase diagram (force equilibrium), a series of fluid displacement patterns can be regarded as capillary force-dominated and viscous force-dominated states. However, from the perspective of the MOPR, a series of fluid displacement patterns can be regarded as displacement states at the

minimum operating power corresponding to the completion of the constant flow displacement task.

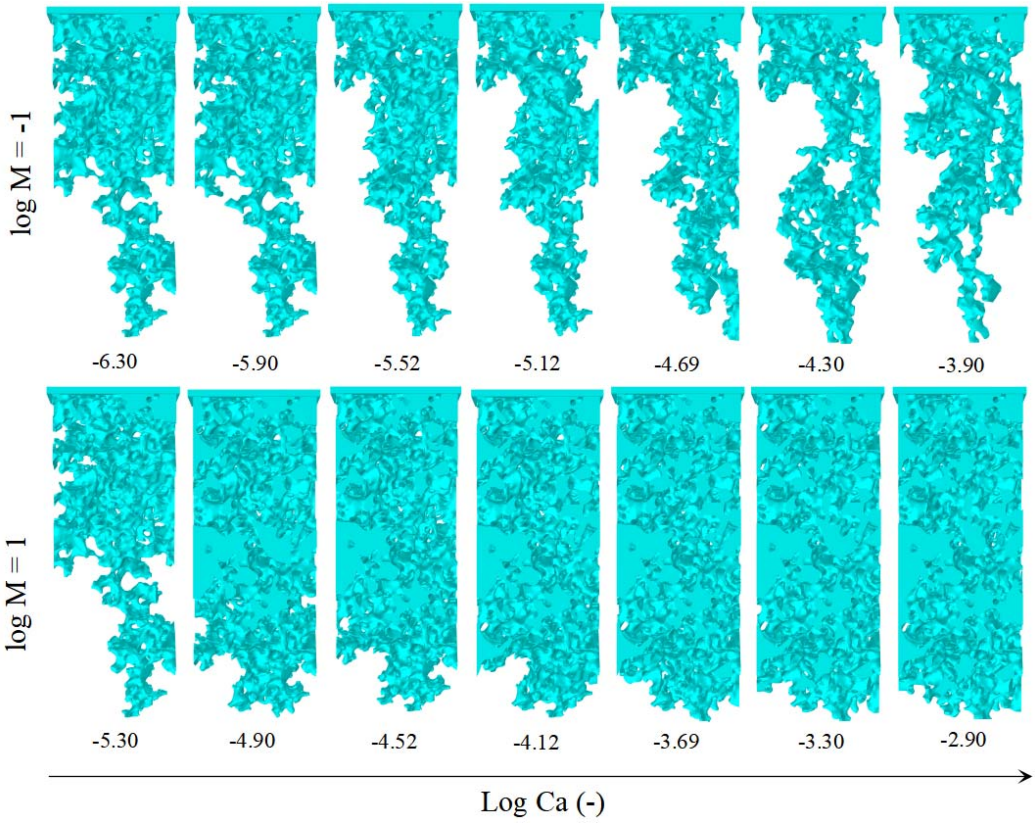

Figure 1. (a) Topological fluid distribution at the breakthrough time. The static contact angle θ^{eq} is set to 95°, which corresponds to weak drainage.

Specifically, for the viscous force-dominated state, the rate of energy introduction into the system by the external pressure difference P_o is approximately equal to the system viscous dissipation rate Φ, the rate of change in the surface energy dF_{surf}/dt and the rate of change in the kinetic energy dE/dt are negligible, and the conversion form of the system operating power P_o can be simplified to $P_o \approx \Phi$. Notably, in such a micron-scale pore system, despite the injection rate v_i being high, the rate of change in the kinetic energy dE/dt (integral term) can be ignored. According to Darcy's law, which is expressed as $\Delta p \approx -\mu LV/k$ (k is the medium permeability and L is the geometric length of the

medium), a fluid phase with a high viscosity flowing through a capillary channel at a constant flow rate has a high viscosity dissipation. Therefore, for the VF state, under the MOPR constraint, the system approaches the minimum operating power state mainly by regulating the viscous dissipation rate of the displaced phase Φ_d. The system minimizes the area of the displacement path of the invading phase to capture a large part of the displaced phase behind the displacement front (the retained phase has a flow rate of 0 and $\Phi_d \to 0$). Although shrinkage of the area of the displacement path of the invading phase can lead to an increase in Φ_i ($A_i \downarrow$, $v_i \uparrow$, and $\Phi_i \uparrow$), the benefit of decreasing Φ_d caused by the increased retention of the displaced phase is far greater than the loss caused by the increase in Φ_i. Moreover, under the constraint of constant flow displacement, part of the displaced phase is always in the migration state, and the system maximizes the area of the migration path of this part of the displaced phase A_d to reduce the viscous dissipation rate of this part ($A_d \uparrow$, $v_d \downarrow$, and $\Phi_d \downarrow$). Therefore, rapid formation of the main displacement path in the macroscopic displacement direction is inevitable for the two-phase flow system to avoid extra work in the VF state. Similarly, for the SD state, the system approaches the minimum operating power state mainly by regulating the viscous dissipation rate of the invading phase Φ_i. That is, the system maximizes the area of the displacement path of the invading phase to reduce the flow velocity of the invading phase, thereby reducing the viscous dissipation rate of the invading phase in the flow region ($A_i \uparrow$, $v_i \downarrow$, and $\Phi_i \downarrow$). Apparently, the loss of the increased Φ_d due to the remigration of the retained displaced phase is much smaller than the benefit of the decreased Φ_i due to the increase in the area of the displacement path of the invading phase. Therefore, the invading phase compactly scans the porous medium, and the formation of secondary flow paths beyond the primary displacement path is inevitable for the two-phase flow system to avoid extra work in the SD state.

In this paper, the mechanism by which the development of the displacement interface in the VF or SD state always follows the displacement path with the minimum viscous dissipation rate is regarded as a self-regulation mechanism of the viscous dissipation rate ($\Phi_i \to \min$ or $\Phi_d \to \min$) and is demonstrated in Fig. 2(a,b). The fluid distributions and velocity field distributions in the VF and SD states and the local velocity distribution of the displaced phase along a cross-section of a porous medium sample are shown. For the VF state, the macroscopic response of the system to the self-regulation mechanism is reflected in the existence of a retention region and a development region of the displaced phase. In the retention region, the local velocity of the displaced phase remains relatively low, while in the development region, the local velocity distribution is uniform and well developed, fluctuating in the range of 0.207 m/s–0.314 m/s. Of course, due to the dendritic structure of the invading fluid in the VF state, there is a clear CZ between the retention and development regions. In the SD state, there is no retention region, only a development region, and the CZ is narrower.

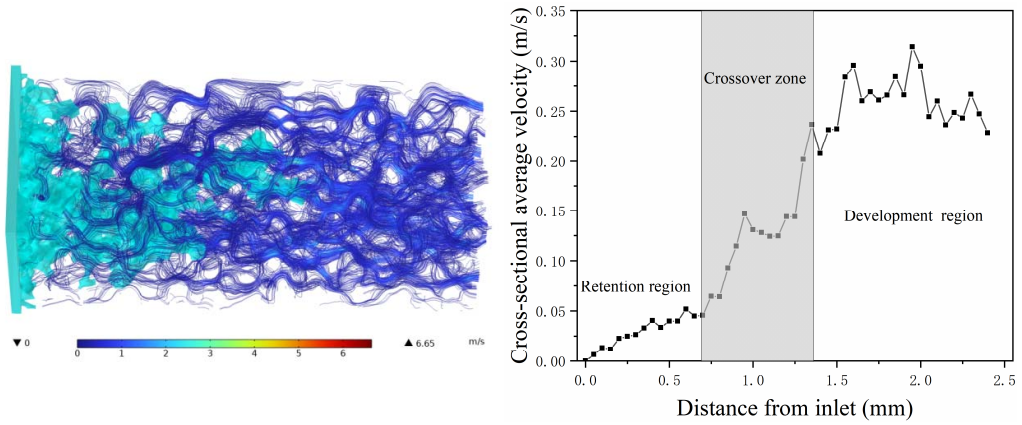

(a)

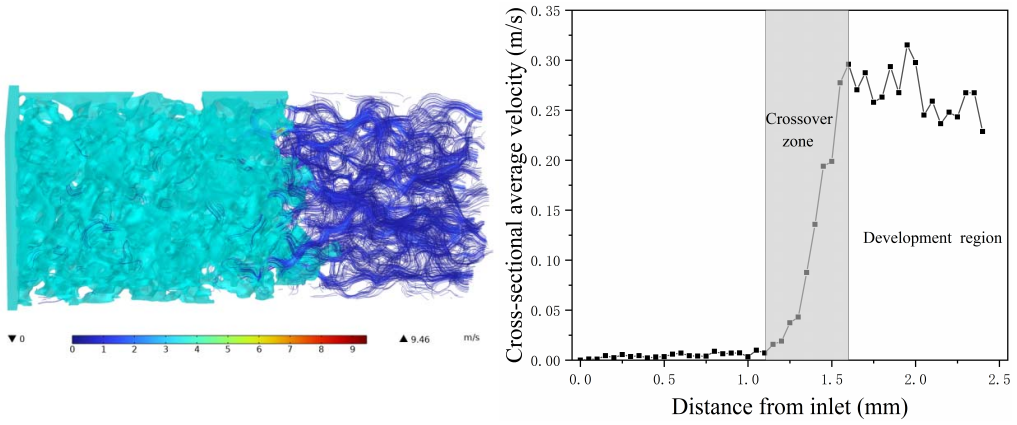

(b)

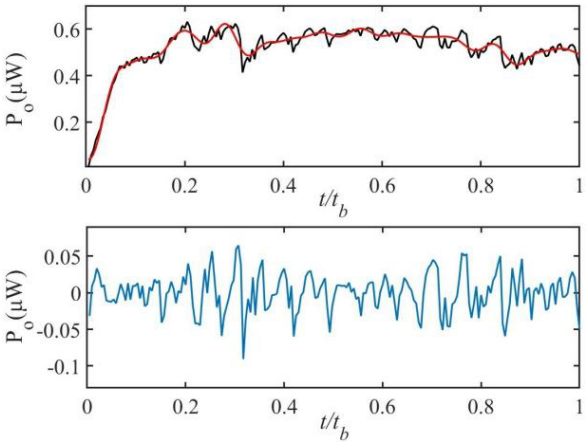

(c)

Figure 2. The fluid distribution of the invading phase and the velocity field distribution of the displaced phase at a certain time (t/t_b = 0.649) under different displacement patterns and the average velocity distribution of the displaced phase along a cross-section of a porous medium sample: (a) VF state (log Ca = -3.90, log M = -1) and (b) SD state (log Ca = -2.90, log M = 1). Low-speed and high-speed flow regions are shown in blue and red, respectively. (c) Evolution characteristics of the operating power P_o in the CF state (log Ca = -4.90) with the normalized time t/t_b, where t is the penetration time and t_b is the breakthrough time ($t \le t_b$). The bottom and top panels show the fluctuating component and the global trend of P_o, respectively.

The decrease in the capillary number Ca changes the relative importance of the viscous and capillary forces, resulting in a transition of the fluid displacement pattern from a viscous force-dominated state to a capillary force-dominated state. In the CF state, the reversible and

255 irreversible capillary force-dominated pore-scale displacement events alternate, which can be
256 demonstrated by the evolution characteristics of the operating power P_o, as shown in Fig. 2(c).
257 In this paper, the operating power signal is decomposed into global trend and fluctuation
258 components using wavelet decomposition (Primkulov et al., 2019). The global
259 low-frequency fluctuation trend of the operating power (red trend line in Fig. 2(c)) corresponds
260 to a reversible displacement event of meniscus invasion into the pore throat under a slow
261 displacement assumption, which is characterized by a uniform slow displacement at all
262 displacement interfaces. The rate of energy introduction P_o by the system pressure drop
263 during reversible displacement is approximately equal to the rate of surface energy change, the
264 viscous dissipation rate Φ and the rate of change in the kinetic energy dE/dt are negligible,
265 and the conversion form of the operating power P_o can be simplified to $P_o \approx dF_{surf}/dt$. That
266 is, P_o is regulated by dF_{surf}/dt, which is controlled by the geometrical structure of the
267 displacement path, which may increase or decrease, resulting in global low-frequency
268 fluctuations of P_o. In the context of the MORP, the system selects the most favorable
269 (minimum energy consumption) displacement path by comparing the rate of the surface
270 energy change of all potential moving menisci in different local pore throat regions.
271 In this paper, the mechanism by which the development of the displacement interface in
272 the CF state always follows the displacement path of the minimum rate of surface energy
273 change is regarded as a self-regulation mechanism of the rate of the surface energy change
274 ($dF_{surf}/dt \to \min$). For a heterogeneous porous medium, deviation of the displacement path
275 from the macroscopic flow direction is clearly inevitable for the system to avoid excess energy
276 consumption, and the benefit from the reduction in dF_{surf}/dt due to the deviation of the
277 displacement path is much greater than the loss due to the possible increases in other energy
278 contribution terms. In addition, the high-frequency oscillations of the operating power P_o are
279 due to the rearrangement of the fluid phase (Haines jumps) as the meniscus migrates from the

narrow pore throat to the wide pore body. Previous studies have suggested that during the Haines jumps, the resulting local velocity is orders of magnitude larger than the injection velocity, which greatly increases the energy dissipation. Clearly, the conversion form of the operating power is also changed, and the viscous dissipation rate Φ can no longer be ignored. The interface reconstruction events, such as Haines jumps, are discussed in Section 2.3.

2.3. Physical origins of the interface reconstruction events

These interface reconfiguration events are generally believed to cause partial driving energy to be converted into viscous dissipated energy, which is a loss of driving energy and can be regarded as an energy-adverse mechanism (Armstrong et al., 2015; Ferrari and Lunati, 2014; O'Brien et al., 2020). However, from the perspective of the MOPR, an interface reconstruction event is an irreversible change between the two most energetically favorable states, and it is an energy favorable self-regulation mechanism derived from the system to avoid additional work under specific constraints. Before an interface reconstruction event, the system is in the most energetically favorable state (minimum surface energy state) under the current constraints because the system follows the displacement path of the minimum rate of surface energy change or the maximum rate of surface energy change. With the changes in the constraints during the displacement process (the increase in the saturation S_i), a metastable fluid configuration is generated. At this moment, any small change in the constraints, such as a slight increase of S_i (reaching a specific constraint condition), may cause the system to no longer be in a minimum surface energy state that satisfies the new constraints, and the fluid topology can be redistributed (via Haines jump, contact or overlap events) to find the new energetically most favorable state, as demonstrated in Fig. 3(a, b), which shows the fluid redistribution associated with interfacial reconstruction events and the evolution characteristics of the associated energy terms during interfacial reconstruction. As shown in Fig. 3(a), during the Haines jump process, the conversion form of the operating power is $P_o + \left| dF_{surf-s}^{rel} / dt \right| = dF_{surf-f} / dt + \Phi + dE/dt$. The sharp decline in the operating power P_o indicates that P_o does not act ($P_0 \to \min$), and the interfacial dynamics are mainly

controlled by $\left|dF_{surf-s}^{rel}/dt\right|$, which is provided by the reverse imbibition of the wetting phase in the adjacent pore throat. Therefore, during a Haines jump, to approach the new minimum surface energy state, the system maximally regulates the fluid topology to force the invading phase to move from a region with a high specific surface area to a region with a low specific surface area (as shown in the inset in Fig. 3(a), the invading phase retreats at the interface in the region with a high specific surface area). Likewise, as shown in Fig. 3(b), for a cooperative pore-filling event during imbibition, the conversion form of the operating power is $\left|dF_{surf-s}^{rel}/dt\right|+\left|dF_{surf-f}/dt\right|=\left|P_0\right|+\Phi+dE/dt$. The energy driving the interface reconstruction mainly originates from the surface energy, and the operating power P_o related to the external pressure difference is not involved. Therefore, during the approach to the new minimum surface energy state, the system maximally forces the invading phase to move from a region with a low specific surface area to a region with a high specific surface area (as shown in the inset in Fig. 3(b), the invading phase retreats at the interface in the region with a low specific surface area). Obviously, the operating power of the termination state of the interface reconfiguration event is far lower than the initial state, and the system reaches a new minimum operating power state.

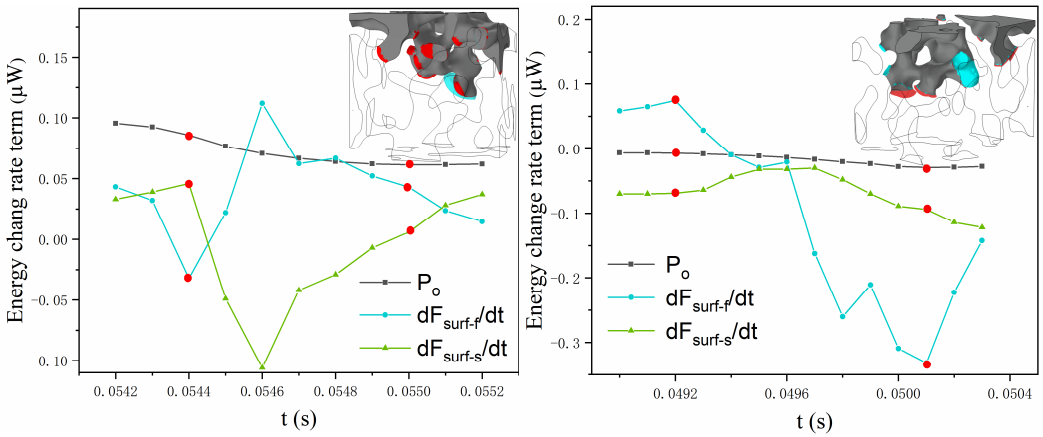

(a) (b)

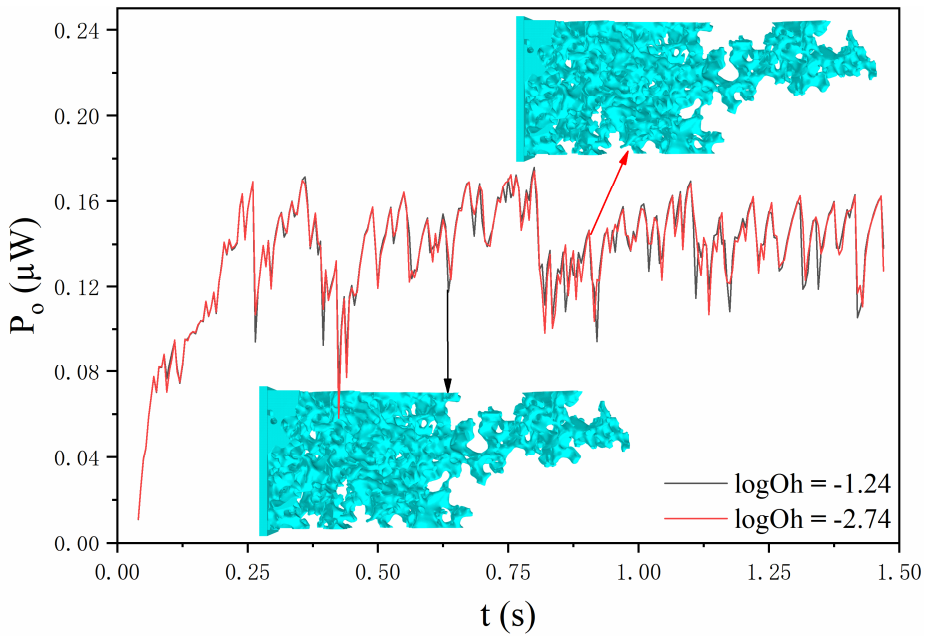

（c）

Figure 3. The dynamic evolutions of P_o, dF_{surf-s}/dt and dF_{surf-s}/dt over time for different interfacial reconstruction events: (a) Haines jump event (θ = 115°), (b) cooperative pore-filling event (θ = 55°). The insets are snapshots of the corresponding fluid redistribution. The area occupied by the invading phase that remained unchanged after the interfacial reconstruction event is shown in gray, the advancing meniscus in the pore body and the receding menisci in the surrounding throats are shown in blue and red, respectively, and the red dots in the curve indicate the start and end of the interface reconstruction event. (c) Operating power P_o as a function of time for different Oh values in the CF state (log Ca = -6.3, log M = -1), where the Ohnesorge number $Oh = \sqrt{Ca/\mathrm{Re}} = \mu_i/\sqrt{\rho_i \sigma d}$ reflects the relative importance of the inertial force to the viscous force and surface tension (in this paper, the fluid density ρ_i is controlled to change Oh while keeping Ca and M constant); d is the characteristic length, which is estimated as $d \approx \pi/S_v$ (75 μm); and S_v is the ratio of the pore-grain interface area to the total volume of the porous medium (Mostaghimi et al., 2020).

In addition, according to several recent studies, during interfacial reconfiguration events, inertial effects can significantly impact fluid invasion patterns in porous media (Zacharoudiou

et al., 2020; Ferrari et al., 2014). However, from the perspective of the MOPR, the minimum surface energy state of the terminal state is only related to the geometric topology and the fluid topology (minimum surface energy state of the initial state) but is not related to the transient dynamics (inertial effects) during the interfacial reconstruction, as demonstrated in Fig. 3(c), which shows the evolution of the operating power P_o with time for different Oh numbers. The overall similar oscillation characteristics of the operating power P_o show that although the Oh number changes by an order of magnitude, the transient dynamics associated with inertial effects do not increase the operating power P_o, and their impact on the macroscopic displacement patterns is very limited (as shown in the inset in Fig. 3(c)).

3. Conclusions

In this study, the minimum operating power principle, which is a fundamental principle governing immiscible fluid flows, provides a convincing physical explanation for many phenomena, including the physical origins of a series of fluid displacement patterns and interfacial reconstruction events. When different constraints are imposed on a two-phase flow system, the self-regulation mechanisms for the control system approaching the minimum operating power state are significantly different. For example, when the self-regulation mechanism of the viscous dissipation rate (for the displaced phase) dominates the displacement process, the system inevitably forms a displaced phase retention region and development region; when the self-regulation mechanism of the viscous dissipation rate (for an invading phase) dominates the displacement process, the system inevitably increases the area of the displacement path of the invading phase; and when the self-regulation mechanism of the rate of surface energy change dominates the displacement process, for heterogeneous porous media, the system inevitably introduces more curved displacement paths. In addition, a series of interface reconstruction phenomena are no longer considered to be adverse energy events that lead to rapid energy dissipation; rather, they are considered to be energy favorable self-regulation mechanisms derived from the system to avoid additional work under specific constraints.

Data Availability Statement

Relevant information of wavelet decomposition can be obtained from https://doi.org/10.5281/zenodo.7439463.

Acknowledgments

This research was funded by the High-level Innovative Talents Program of Hebei University (521100221059).

References

Singh K, Jung M, Brinkmann M, et al. Capillary-dominated fluid displacement in porous media[J]. Annual Review of Fluid Mechanics, 2019, 51: 429-449.

Holtzman R, Segre E. Wettability stabilizes fluid invasion into porous media via nonlocal, cooperative pore filling[J]. Physical review letters, 2015, 115(16): 164501.

Zhao B, MacMinn C W, Juanes R. Wettability control on multiphase flow in patterned microfluidics[J]. Proceedings of the National Academy of Sciences, 2016, 113(37): 10251-10256.

Jiang F, Tsuji T. Impact of interfacial tension on residual CO_2 clusters in porous sandstone[J]. Water Resources Research, 2015, 51(3): 1710-1722.

Zacharoudiou I, Boek E S, Crawshaw J. Pore-Scale Modeling of Drainage Displacement Patterns in Association With Geological Sequestration of CO_2[J]. Water Resources Research, 2020, 56(11): e2019WR026332.

Rokhforouz M R, Amiri H A A. Effects of grain size and shape distribution on pore-scale numerical simulation of two-phase flow in a heterogeneous porous medium[J]. Advances in Water Resources, 2019, 124: 84-95.

Lenormand R, Touboul E, Zarcone C. Numerical models and experiments on immiscible displacements in porous media[J]. Journal of fluid mechanics, 1988, 189: 165-187.

Cieplak M, Robbins M O. Influence of contact angle on quasistatic fluid invasion of porous media[J]. Physical Review B, 41(16), 11508 (1990).

Basirat F, Yang Z, Niemi A. Pore-scale modeling of wettability effects on CO_2-brine displacement during geological storage[J]. Advances in water resources, 109, 181-195 (2017).

Lin W, Xiong S, Liu Y, et al. Spontaneous imbibition in tight porous media with different wettability: Pore-scale simulation[J]. Physics of Fluids, 32(3), 032013 (2021).

Jahanbakhsh A, Shahrokhi O, et al. Understanding the role of wettability distribution on pore-flling and displacement patterns in a homogeneous structure via quasi 3D pore-scale modelling[J]. Scientifc Reports, 11, 17847 (2021).

Jung M, Brinkmann M, Seemann R, et al. Wettability controls slow immiscible displacement through local interfacial instabilities[J]. Physical Review Fluids, 1(7), 074202 (2016).

Hu R, Wan J, Yang Z, et al. Wettability and flow rate impacts on immiscible displacement: A theoretical model[J]. Geophysical Research Letters, 2018, 45(7): 3077-3086.

Chen Y, Valocchi A J, Kang Q, et al. Inertial effects during the process of supercritical CO_2 displacing brine in a sandstone: Lattice Boltzmann simulations based on the continuum-surface-force and geometrical wetting models[J]. Water Resources Research, 2019, 55(12): 11144-11165.

Zacharoudiou I, Boek E S. Capillary filling and Haines jump dynamics using free energy Lattice Boltzmann simulations[J]. Advances in water resources, 2016, 92: 43-56.

Berg S, Ott H, Klapp S A, et al. Real-time 3D imaging of Haines jumps in porous media flow[J]. Proceedings of the National Academy of Sciences, 2013, 110(10): 3755-3759.

Hu R, Wu D S, Yang Z, et al. Energy conversion reveals regime transition of imbibition in a rough fracture[J]. Geophysical Research Letters, 2018, 45(17): 8993-9002.

Xu G, Zhao L, Yang C T. Derivation and verification of minimum energy dissipation rate principle of fluid based on minimum entropy production rate principle[J]. International Journal of Sediment Research, 2016, 31(1): 16-24.

Huang H Q, Chang H H, Nanson G C. Minimum energy as the general form of critical flow and maximum flow efficiency and for explaining variations in river channel pattern[J]. Water Resources Research, 2004, 40(4).

Nanson G C, Huang H Q. Least action principle, equilibrium states, iterative adjustment and the stability of alluvial channels[J]. Earth Surface Processes and Landforms: The Journal of the British Geomorpholog ical Research Group, 2008, 33(6): 923-942.

425 Jansen J D, Nanson G C. Anabranching and maximum flow efficiency in Magela Creek, northern
426 Australia[J]. Water Resources Research, 2004, 40(4).
427 Guo X, Liu R, Wang J, et al. Pore-scale modeling of wettability effects on infiltration behavior in
428 liquid composite molding[J]. Physics of Fluids, 2020, 32(9): 093311.
429 COMSOL Multiphysics® v. 5.4. COMSOL AB. Retrieved from www.comsol.com
430 Primkulov B K, Pahlavan A A, Fu X, et al. Signatures of fluid–fluid displacement in porous
431 media: wettability, patterns and pressures[J]. Journal of Fluid Mechanics, 2019, 875.
432 Armstrong R T, Evseev N, Koroteev D, et al. Modeling the velocity field during Haines jumps in
433 porous media[J]. Advances in Water Resources, 2015, 77: 57-68.
434 Ferrari A, Lunati I. Inertial effects during irreversible meniscus reconfiguration in angular pores[J].
435 Advances in water resources, 2014, 74: 1-13.
436 O'Brien A, Afkhami S, Bussmann M. Pore-scale direct numerical simulation of Haines jumps in a
437 porous media model[J]. The European Physical Journal Special Topics, 2020, 229(10):
438 1785-1798.
439 Mostaghimi P, Bijeljic B, Blunt M J. Simulation of flow and dispersion on pore-space images[J].
440 SPE Journal, 2012, 17(04): 1131-1141.
441